MOLECULAR ECOLOGY

Molecular Ecology (2012) **21**, 2502–2518 doi: 10.1111/j.1365-294X.2012.05512.x

Comprehensive sampling reveals circumpolarity and sympatry in seven mitochondrial lineages of the Southern Ocean crinoid species *Promachocrinus kerguelensis* (Echinodermata)

L. G. HEMERY,* M. ELÉAUME,* V. ROUSSEL,† N. AMÉZIANE,* C. GALLUT,‡ D. STEINKE,§ C. CRUAUD,¶ A. COULOUX¶ and N. G. WILSON**

**Muséum national d'Histoire naturelle, Département des Milieux et Peuplements Aquatiques, UMR 7208, CP26, 57 rue Cuvier, 75231 Paris Cedex 05, France, †Muséum national d'Histoire naturelle, Département des Milieux et Peuplements Aquatiques, UMR 7208, Station de Biologie Marine, Place de la Croix, BP 225, 29182 Concarneau Cedex, France, ‡Muséum national d'Histoire naturelle, Département Systématique et Évolution, UMR 7138, CP26, 57 rue Cuvier, 75231 Paris Cedex 05, France, §Biodiversity Institute of Ontario, University of Guelph, 50 Stone Road East, Guelph, Ontario, Canada N1G 2W1, ¶Genoscope, Centre National de Séquençage, 2 rue Gaston Crémieux, CP5706, 91057 Évry Cedex, France, **The Australian Museum, 6 College Street, Sydney, NSW 2010, Australia*

Abstract

Sampling at appropriate spatial scales in the Southern Ocean is logistically challenging and may influence estimates of diversity by missing intermediate representatives. With the assistance of sampling efforts especially influenced by the International Polar Year 2007–2008, we gathered nearly 1500 specimens of the crinoid species *Promachocrinus kerguelensis* from around Antarctica. We used phylogeographic and phylogenetic tools to assess its genetic diversity, demographic history and evolutionary relationships. Six phylogroups (A–F) identified in an earlier study are corroborated here, with the addition of one new phylogroup (E2). All phylogroups are circumpolar, sympatric and eurybathic. The phylogeny of *Promachocrinus* phylogroups reveals two principal clades that may represent two different cryptic species with contrasting demographic histories. Genetic diversity indices vary dramatically within phylogroups, and within populations, suggesting multiple glacial refugia in the Southern Ocean: on the Kerguelen Plateau, in the East Weddell Sea and the South Shetland Islands (Atlantic sector), and on the East Antarctic continental shelf in the Dumont d'Urville Sea and Ross Sea. The inferences of gene flow vary among the phylogroups, showing discordant spatial patterns. Phylogroup A is the only one found in the Sub-Antarctic region, although without evident connectivity between Bouvet and Kerguelen populations. The Scotia Arc region shows high levels of connectivity between populations in most of the phylogroups, and barriers to gene flow are evident in East Antarctica.

Keywords: Antarctica, crinoid, cryptic species, gene flow, haplotype diversity, refugia

Received 11 September 2011; revision received 10 January 2012; accepted 25 January 2012

Introduction

Recent genetic studies on benthic invertebrates from the Southern Ocean have revealed unexpected diversity in many study organisms. Putative cryptic species have been recovered in Mollusca (Linse *et al.* 2007; Wilson *et al.* 2009; Allcock *et al.* 2011), Arthropoda (Held 2003; Held & Wagele 2005; Raupach & Wagele 2006; Raupach *et al.* 2007; Leese & Held 2008; Brandao *et al.* 2010; Krabbe *et al.* 2010; Baird *et al.* 2011; Havermans *et al.* 2011), Echinodermata (Wilson *et al.* 2007; Hunter & Halanych 2008, 2010; Heimeier *et al.* 2010), Annelida (Schüller 2011) and Nemerta (Thornhill *et al.* 2008).

Correspondence: Lenaïg G. Hemery, Fax: 33140793771; E-mail: lhemery@mnhn.fr

Most of these species were thought to show a circumpolar and/or eurybathic distribution, which means that most distributional data in the Southern Ocean must be treated with caution. As Knowlton (1993, 2000) predicted for all marine habitats, an increase in sampling effort, and the application of genetic tools, could reveal more cryptic species in the Southern Ocean.

Many of the cryptic species discovered in the Southern Ocean are partitioned by depth (Raupach *et al.* 2007; Brandao *et al.* 2010; Schüller 2011) or geography (Held & Wagele 2005; Raupach & Wagele 2006; Linse *et al.* 2007; Hunter & Halanych 2008; Thornhill *et al.* 2008; Brandao *et al.* 2010; Krabbe *et al.* 2010). This seems counterintuitive in the light of large homogenizing currents, such as the Antarctic Circumpolar Current (ACC), and a lack of obvious physical barriers around Antarctica. However, if organisms lack free-swimming larvae, or any other mechanism to disperse at a large scale, even weak barriers to gene flow could result in allopatric speciation.

The Southern Ocean is known to have undergone a succession of glaciations for millions of years, with large extensions of grounded ice sheets on the Antarctic continental shelf followed by asynchronous retreats (see reviews in Clarke & Crame 1992, 2010; Thatje *et al.* 2005). This succession is thought to be the climatic response to the Milankovitch cyclic variability, driving perhaps the strongest evolutionary force for both the Antarctic terrestrial and marine flora and fauna (Clarke & Crame 1992, 2010). Thatje *et al.* (2005, 2008) hypothesized that vicariant speciation could have occurred on the Antarctic continental shelf, within multiple refugia left free of grounded ice sheets. The extant Antarctic benthic fauna is thought to be the result of both migration and vicariance, a result of the so-called Antarctic biodiversity pump (Clarke & Crame 1992, 2010). During times of ice shelf retreat, barriers to gene flow were removed allowing for secondary contact between vicarious lineages (Thatje *et al.* 2005, 2008; Thornhill *et al.* 2008; Heimeier *et al.* 2010; Havermans *et al.* 2011).

Among the benthic invertebrates suspected to consist of a cryptic species, complex is the crinoid *Promachocrinus kerguelensis* (Carpenter 1888). It is the most abundant crinoid in the Southern Ocean (Marr 1963; Clark & Clark 1967; Speel & Dearborn 1983; Eléaume 2006) and is known from the whole Antarctic continental shelf to Sub-Antarctic islands such as Crozet and Kerguelen, and even to the Campbell Plateau, south of New Zealand (black circles in Fig. 1), at depths ranging from 20 m to 2100 m (Speel & Dearborn 1983). This crinoid is thought to have large dispersal potential as it produces positively buoyant lecithotrophic larvae that are predicted to stay within the plankton for several weeks or months (McClintock & Pearse 1987). Applying genetic analysis tools to a range of samples from within the Atlantic sector of Antarctica, Wilson *et al.* (2007) recognized six distinct lineages. No evidence for a correlation between morphological characters from these specimens and these genetic lineages could be found (Eléaume 2006), suggesting that they could represent cryptic species.

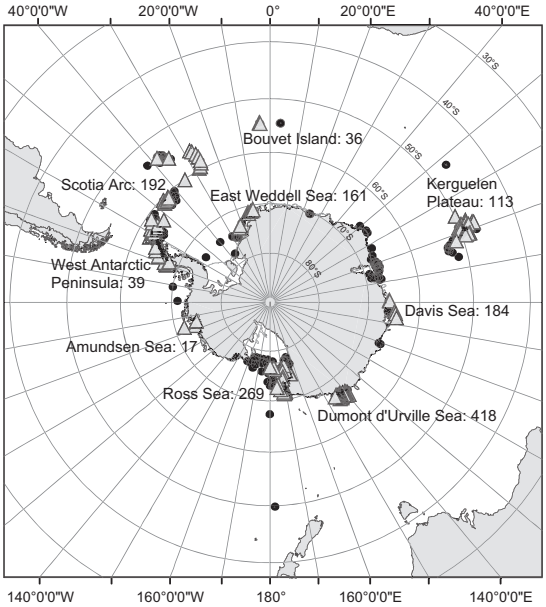

Fig. 1 *Promachocrinus kerguelensis* sampling stations in the Southern Ocean. Triangles, sampled stations; circles, bibliographic data; numbers, sequenced specimens per region.

Our study was designed to improve spatially scaled sampling to test whether the known genetic lineages in *P. kerguelensis* represent an under-sampling artefact of a large and genetically diverse population, or whether they are truly representative of the Southern Ocean. We explored the evolutionary relationships among the lineages, by re-examining their phylogeny with a larger data set, and using a sampling strategy guided by population analyses to encompass the broadest possible genetic variation. We also wanted to understand the distributional limits of each phylogroup in *P. kerguelensis* to assess the connectivity displayed throughout their range, and to test the 'multiple refugia' theory by studying the demographic history of each phylogroup.

Materials and methods

Sampling

A total of 1307 specimens of *Promachocrinus kerguelensis* were selected for sequencing among more than 2500 specimens collected. Most of these were sampled during

Antarctic and Sub-Antarctic surveys from 1996 to 2010, with increased sampling effort facilitated by the last International Polar Year (IPY, 2006–2008). Specimens were collected in eight general regions: Kerguelen Plateau (KP), Davis Sea (DS), Dumont d'Urville Sea (DDU), Ross Sea (RS), Amundsen Sea (AS), West Antarctic Peninsula (WAP), East Weddell Sea (EWS) and Scotia Arc (SA) including the tip of the Antarctic Peninsula and the Bransfield Strait. Sampling regions are shown in Fig. 1 (triangles), and details of cruises are summarized in Table 1. Specimens were fixed and preserved in 70–95% ethanol or first frozen and subsequently preserved in ethanol. Some morphological traits were recorded during sorting: colour (brown, yellow, purple), pattern (plain, striped, spotted) and the number of pairs of arms (6–11). Voucher specimens have been deposited at several museums and institutes. The full details of repository and station data are listed in Table S1 (Supporting information) and can be found in the Barcode of Life Data System (BOLD, http://www.boldsystems.org, see Ratnasingham & Hebert 2007) listed in the public project PROKE. Hundred and twenty-two additional *P. kerguelensis* cytochrome c oxidase subunit I (COI) sequences were obtained from GenBank (DQ823236 to DQ823349) from Wilson *et al.* (2007), covering the WAP and SA areas and a ninth area around Bouvet Island (BI).

DNA extraction, PCR and sequencing

Molecular procedures were conducted in several institutions (CCDB, SSM and SIO, see acknowledgments for acronym details). Work carried out at the CCDB followed the DNA extraction protocol described in Ivanova *et al.* (2006) and the PCR protocol in Eléaume *et al.* (2011). At SSM, DNA was extracted using Qiagen QIAmp DNA Tissue Micro Kit with modifications to the manufacturer's instructions; proteinase K was increased to 30 μL, buffer AL increased to 300 μL, 100% ethanol increased to 400 μL and eluting with 50 μL buffer AE. DNA was amplified by PCR and bidirectionally sequenced by the Génoscope (Evry, France). PCR products from SIO were bidirectionally sequenced by ASGPB (University of Hawaii at Manoa) or Génoscope; 554 bp of the barcode region of COI was amplified using the Folmer *et al.* (1994) primers LCO1490 and HCO2198 and a new crinoid-specific forward primer LH-CO1F2 (Table 2), and following cycling conditions: 94 °C 2 min, 40 × [94 °C 1 min, 46 °C 2 min, 72 °C 3 min], 72 °C 5 min. Four other genes were sequenced for 23 specimens of *P. kerguelensis* and two outgroups. A 673-bp fragment of cytochrome b (Cytb) was amplified using specific primers, LH-cytbF2 and LH-cytbR979, (Table 2) and following cycling conditions: 94 °C 4 min, 40 × [94 °C 40 s, 45 °C 45 s, 72 °C 1 min] and 72 °C 10 min. A 311-bp fragment of 16S rDNA was amplified using specific primers LH-16SF1 and LH-16SR1 (Table 2) and following cycling conditions: 94 °C 4 min, 40 × [94 °C 40 s, 53 °C 40 s, 72 °C 1 min] and 72 °C 10 min. A 743-bp fragment of 28S rDNA was amplified using specific primers LH-28SF1 or LH-28SF3 and LH-28SR1 or LH-28SR3 (Table 2) and following cycling conditions: 94 °C 4 min, 40 × [94 °C 40 s, 54–57 °C 40 s, 72 °C 1 min] and 72 °C 10 min. A 736-bp

Table 1 Cruises from which *Promachocrinus kerguelensis* were collected for this study

Area	Cruise	Vessel	Year
Amundsen Sea	BIOPEARL II (JR179)	RV *James Clark Ross*	2008
Davis Sea	BR09	RV *Aurora Australis*	2009–2010
Dumont D'Urville Sea	CEAMARC (2007/08 V3)	RV *Aurora Australis*	2007–2008
East Weddell Sea	EASIZ I (ANT XIII/3)	RV *Polarstern*	1996
	EASIZ III (ANT XVII/3)	RV *Polarstern*	2000
	BENDEX (ANT XXI/2)	RV *Polarstern*	2003–2004
	ANDEEP III (ANT XXII/3)	RV *Polarstern*	2005
Kerguelen Plateau	HIMI-SC50	FV *Southern Champion*	2008
	POKER II	*Austral*	2010
Ross Sea	ITALICA 2004	RV *Italica*	2004
	TAN0402	RV *Tangaroa*	2004
	TAN0802	RV *Tangaroa*	2008
Scotia Arc	EASIZ III (ANT XVII/3)	RV *Polarstern*	2000
	ANDEEP I&II (ANT XIX/3&4)	RV *Polarstern*	2002
	LAMPOS (ANT XIX/5)	RV *Polarstern*	2002
	BIOPEARL I (JR147)	RV *James Clark Ross*	2006
	AMLR 2009, Leg II	RV *Yuzhmorgeologiya*	2009
West Antarctic Peninsula	BASWAP (JR230)	RV *James Clark Ross*	2009
	AMLR 2009, Leg II	RV *Yuzhmorgeologiya*	2009

Table 2 New crinoid-specific primers used to amplify the COI, Cytb, 16S and 28S markers

Primer name	Primer sequence
LH-COIF2	5′-ACRAATCATAAGGATATWGGDACTT-3′
LH-cytbF2	5′-TGCATTACACAGCTGATATA-3′
LH-cytbR979	5′-TATCAYTCYGGTTGTATRTGAAC-3′
LH-16SF1	5′-AGATAGAAACTGACCTGACTT-3′
LH-16SR1	5′-TTAAGCTCGACAGGGTCTT-3′
LH-28SF1	5′- AGCATATTACTAAGCGGAG-3′
LH-28SF3	5′-GGATCAGCCCAGCGCCGAAT-3′
LH-28SR1	5′-CGCAATGAAAGTGAAGGC-3′
LH-28SR3	5′-TAGACTCCTTGGTCCGTGTTTC-3′

COI, cytochrome *c* oxidase subunit I.

fragment of ITS (including ITS1-5.8S-ITS2) was amplified using the Cohen *et al.* (2004) primers and following cycling conditions: 94 °C 4 min, 40 × [94 °C 40 s, 57 °C 40 s, 72 °C 1 min] and 72 °C 10 min. The sequence quality was checked using Sequencher v4.1.4 (Gene Codes Corporation, Ann Arbor, USA). The sequences were aligned manually using BioEdit Sequence Alignment Editor v7.0.9.0 (Hall 1999) and translated into amino acid sequences using the echinoderm mitochondrial genetic code in MEGA5 (Tamura *et al.* 2011) to check for possible stop codons.

Haplotype networks and barcoding analyses

Haplotype networks were generated using TCS 1.21 (Clement *et al.* 2000) under the criterion of statistical parsimony. A first network was generated with the full COI data set. Reticulations were resolved by applying the coalescent predictions outlined by Posada & Crandall (2001) (Fig. 2; less probable reticulation converted to dashed lines). Then, 23 specimens were selected and sequenced for other genes. They were chosen from the four most sampled areas (DDU, RS, EWS and SA) to represent at least one specimen from the most frequent COI haplotypes and some additional unique COI haplotypes. To compare mitochondrial and nuclear results, six haplotype networks from this subset (COI; Cytb; COI + Cytb; ITS; 28S; ITS + 28S) were generated. The proportion of individual assignation of mitochondrial phylogroups to nuclear phylogroups was calculated. Uncorrected pairwise distances (p-dist) were calculated in MEGA5 within and among phylogroups defined according to the haplotype networks, but also within pairs of phylogroups. The latter were used to calculate barcode-gaps (Meyer & Paulay 2005) among every pair of phylogroups. To test for possible selection in the divergence between phylogroups, a McDonald–Kreitman test (MK) was performed in DnaSP 5.10.01 (Librado & Rozas 2009) between each pair of closely related phylogroups in the haplotype network (A–D; B–C; C–D; D–E1; D–F; E1–E2, E1–F).

Phylogenetic analyses

The same 23 specimens selected for the network comparisons were used for evolutionary analysis via a multilocus phylogenetic approach (COI, Cytb, 16S, 28S and

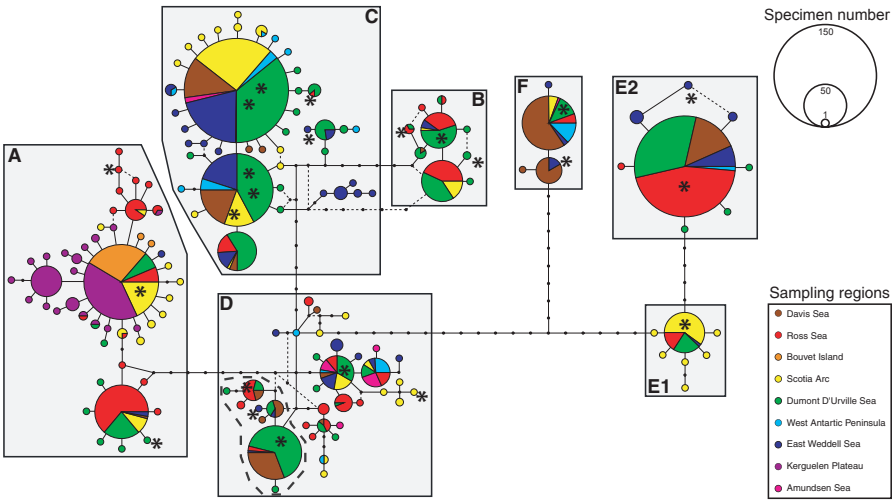

Fig. 2 Cytochrome *c* oxidase subunit I haplotype network of *Promachocrinus kerguelensis*. Boxes are networks obtained with a 99% connection limit in TCS; thick dashed line represents haplotypes shared by all 'six-radialed' specimens; thin dashed lines are resolved reticulations; stars show haplotypes for which a specimen was also sequenced for Cytb, 16S, ITS and 28S.

ITS). Maximum likelihood (ML) analyses were used to estimate the relationships between phylogroups defined by phylogeographic analyses. The two outgroups were a Heliometrinae species *Anthometrina adriani* (Bell 1908) and a Notocrinidae species *Notocrinus virilis* Mortensen 1917;. The best evolutionary model according to Treefinder (Jobb 2008) was selected using the AIC criterion for each gene: GTR + I + G for COI, J2 + I + G for Cytb, GTR + G for 16S, J1 + G for 28S and J2 + G for ITS. First, each gene was treated separately with ML analyses conducted in Treefinder, using the selected models without codon partitioning, as well as bootstrapping (1000 iterations) to estimate node support. The trees obtained (results not shown) were compared by eye looking for incongruent but well-supported nodes. Congruent data sets were combined in an unlinked-partition data set, followed by ML analysis with bootstrapping (1000 iterations) using the appropriate model for each partition.

Population genetics and demographic analyses

First, we considered that groups defined by the network analyses represented different phylogroups, and subsequent comparisons were made only within each of these phylogroups. To define populations within regions for each phylogroups, we first calculated pairwise F_{ST} in ARLEQUIN v.3.5.1.2 (Excoffier & Lischer 2010) between all sampling stations with more than five specimens. Regions are as shown in Fig. 1, with the exception that the Scotia Arc was further subdivided into South Shetland Islands (SSh), South Orkney Islands (SO), South Sandwich Islands (SSa) and South Georgia (SG); and the EWS sampling area was subdivided into Kapp Norvegia (EWS1) and Halley Bay (EWS2). As the pairwise F_{ST} comparisons within each geographical region were not significantly different from zero (results not shown), sampling stations within each region were pooled together to form what we defined as populations (Fig. S1, Supporting information). For each population, we then calculated haplotypic diversity (Hd), nucleotide diversity (π), average number of nucleotide differences (θ_π) and average number of polymorphic sites (θ_S) using ARLEQUIN. The number of 'private alleles' was also calculated following Maggs *et al.* (2008) methods to assess the existence of past glacial refugia. We explored neutrality of nucleotide variation and population demographics for each population using Fu's F_S statistics generated in ARLEQUIN, with significance tested by 1000 permutations. Distributions of pairwise differences (mismatch distribution) were generated for each population using ARLEQUIN. To assess levels of genetic differentiation among populations, we estimated pairwise F_{ST} and Φ_{ST} (implementing the Tamura model [Tamura 1992] without gamma correction, selected using Treefinder) in ARLEQUIN.

Results

Defining phylogroup-level diversity

A total of 1429 COI sequences from nine sampling areas were included in this analysis (Figs 1 and 2). This data set showed 108 polymorphic sites defining 154 haplotypes in TCS, whereas the reduced COI data set of 23 individuals showed 63 polymorphic sites defining 20 haplotypes. The 610-bp alignment of Cytb from the same 23 specimens showed 83 polymorphic sites defining 16 haplotypes, and when combined to a single mitochondrial locus, the 1154-bp alignment of COI + Cytb showed 146 polymorphic sites defining 21 haplotypes. The 707-bp alignment of ITS showed 35 polymorphic sites defining 13 haplotypes, the 743-bp alignment of 28S showed three polymorphic sites defining three haplotypes, and when combined to a single nuclear locus, the 1450-bp alignment of ITS + 28S showed 38 polymorphic sites defining 14 haplotypes.

Using default parameters in TCS (connection threshold of 95%) on the reduced separate data sets for COI, Cytb and ITS resulted in four, six and two disconnected networks, respectively, and only one network for 28S (A, B + C + D, E1 + E2 and F for COI; A, B + C, D, E1, E2 and F for Cytb; α and β for ITS; $\alpha + \beta$ for 28S; Fig. 3, named A–F following Wilson *et al.* 2007 with the addition of the newly discovered E2 phylogroup on mitochondrial networks). When combined into a single mitochondrial (COI + Cytb) or nuclear (ITS + 28S) data set, the default connection limit (95%) produced nine (A, B, C, E1, E2, F, and splitting D into three disconnected networks) and two (α and β) networks, respectively (Fig. 3). When the full COI data set was subjected to statistical parsimony in TCS (95%), it formed three disconnected haplotype networks (A + B + C + D, E1 + E2 and F; Fig. 2). If the 99% threshold was applied, four more networks were disconnected, separating A, B, C and D from each other, and E1 from E2. There was a perfect individual assignation of mitochondrial phylogroups to nuclear phylogroups, with nuclear clade α including 100% of mitochondrial phylogroups A–D and nuclear clade β including 100% of mitochondrial phylogroups E–F. The seven COI networks were considered as different phylogroups for the rest of the analyses (boxes in Fig. 2).

Uncorrected pairwise distances were calculated between phylogroups. Intragroup uncorrected pairwise distances (0.04–0.68%) (Table 3) were always smaller than intergroup distances (1.16–6.12%). E1 and E2 presented the lowest intergroup variation (1.16%) and

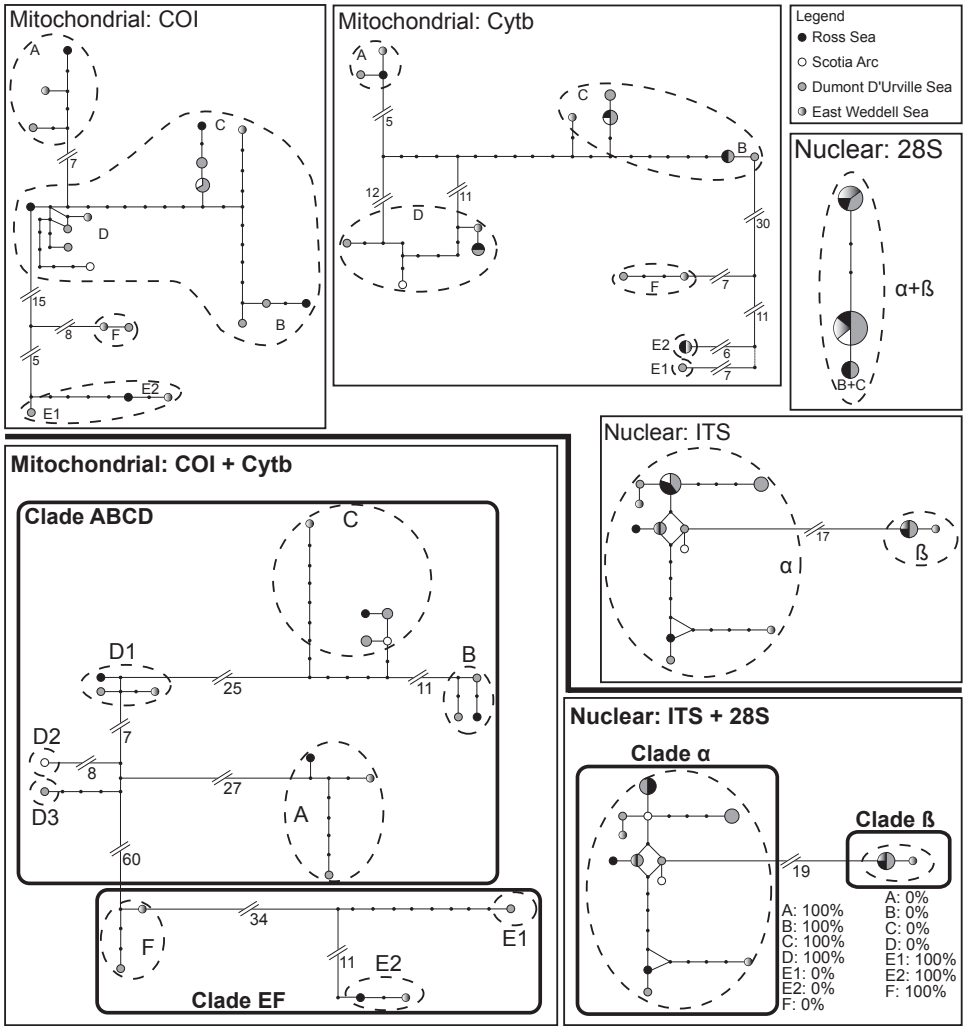

Fig. 3 Comparison of separate and combined haplotype networks of *Promachocrinus kerguelensis* produced using 23 sequences of two mitochondrial (cytochrome c oxidase subunit I and Cytb) and two nuclear (ITS and 28S) genes. Dashed line indicates networks obtained with a 95% connection limit in TCS; A–F, mitochondrial phylogroup names; α-β, nuclear phylogroup names; thick boxes indicate retained clades; numbers next to the ITS + 28S clades are per cent of individual assignation of mitochondrial phylogroups to nuclear phylogroups.

showed the smallest intragroup variation (~0.05%). Plotting p-distance frequencies, a clear 'barcode-gap' was found for nearly every pair of groups (Fig. 4). Only three comparisons (A–D, B–C and C–D) did not show a clear barcode-gap.

No fixed nonsynonymous substitutions between phylogroups A–D, B–C, C–D, E1–E2, E1–F, and two fixed nonsynonymous substitutions between phylogroups D–E1 and D–F were found. The MK test was never significant, whatever the pairs of phylogroups tested. The null hypothesis could not be rejected, and the data were considered consistent with the neutral hypothesis, indicating that the observed COI haplotype diversification was not owing to positive (ecological) selection but rather reflected demographic history.

Maximum likelihood trees obtained for each gene produced congruent topologies (data not shown), and all data sets were combined to obtain a concatenated multigene phylogenetic tree (Fig. 5). The node corresponding to the ingroup species *Promachocrinus kerguelensis* was supported by high bootstrap values and showed two monophyletic lineages (Clades 1 and 2). Clade 1 consisted of phylogroups A + (B + C) + D in a polytomy, and Clade 2 consisted of two sister clades

Table 3 Average uncorrected pairwise distances (p-dist, in %) and standard deviation within (in bold) and between phylogroups of *Promachocrinus kerguelensis*

	A	B	C	D	E1	E2	F
A	**0.44 ± 0.15**						
B	3.49 ± 0.73	**0.16 ± 0.10**					
C	3.06 ± 0.70	1.76 ± 0.50	**0.36 ± 0.12**				
D	2.53 ± 0.61	3.10 ± 0.65	2.06 ± 0.51	**0.68 ± 0.21**			
E1	5.11 ± 0.87	5.40 ± 0.90	4.99 ± 0.86	4.32 ± 0.79	**0.05 ± 0.02**		
E2	5.84 ± 1.00	6.12 ± 1.00	5.62 ± 0.97	4.93 ± 0.89	1.16 ± 0.43	**0.04 ± 0.02**	
F	5.46 ± 0.91	5.61 ± 0.92	4.92 ± 0.85	4.61 ± 0.80	2.76 ± 0.67	3.47 ± 0.75	**0.09 ± 0.08**

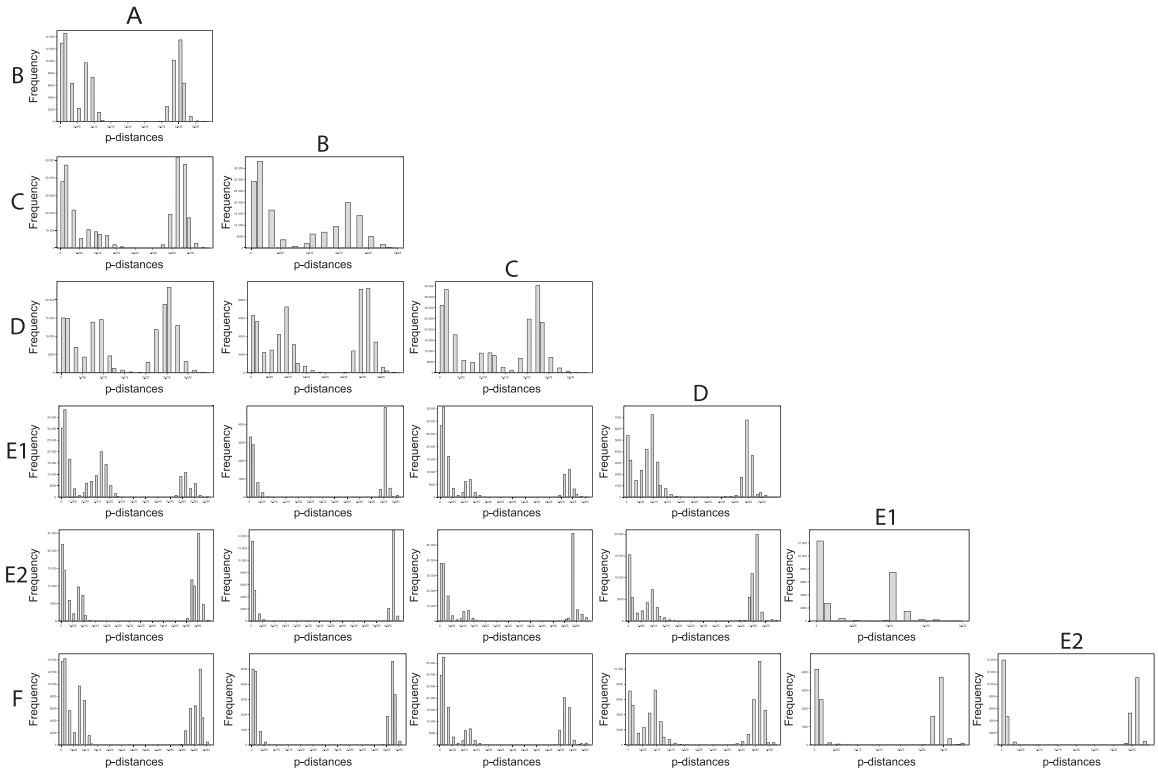

Fig. 4 Histograms of pairwise p-distance frequencies showing barcode-gaps between each pair of phylogroups of *Promachocrinus kerguelensis*.

(E1 + E2) + F. Nodes corresponding to each haplotype network were highly supported, except for phylogroup C, which was paraphyletic, with the well-supported phylogroup B nested inside it.

Phylogroup distributions and morphology

All phylogroups occurred in at least six sampling areas on the Antarctic continental shelf and the Scotia Arc (Fig. 6). However, only phylogroup A was found in the Sub-Antarctic Bouvet and Kerguelen areas (Figs 2 and 6). All phylogroups were sympatric in three localities (DDU, EWS1 and RS), and six phylogroups were found together in two additional localities (DS and SSh).

All phylogroups displayed overlapping bathymetrical ranges. Phylogroup A was found from 106 to 541 m; B from 147 to 1157 m; C from 65 to 1170 m; D from 147 to 1170 m; E1 from 147 to 525 m; E2 from 147 to 1157 m; and F from 176 to 1157 m. All phylogroups occurred in <200 m, and >1000 m, with the exception of phylogroups A and E1. In localities where phylogroups were sympatric, the depth ranges overlapped.

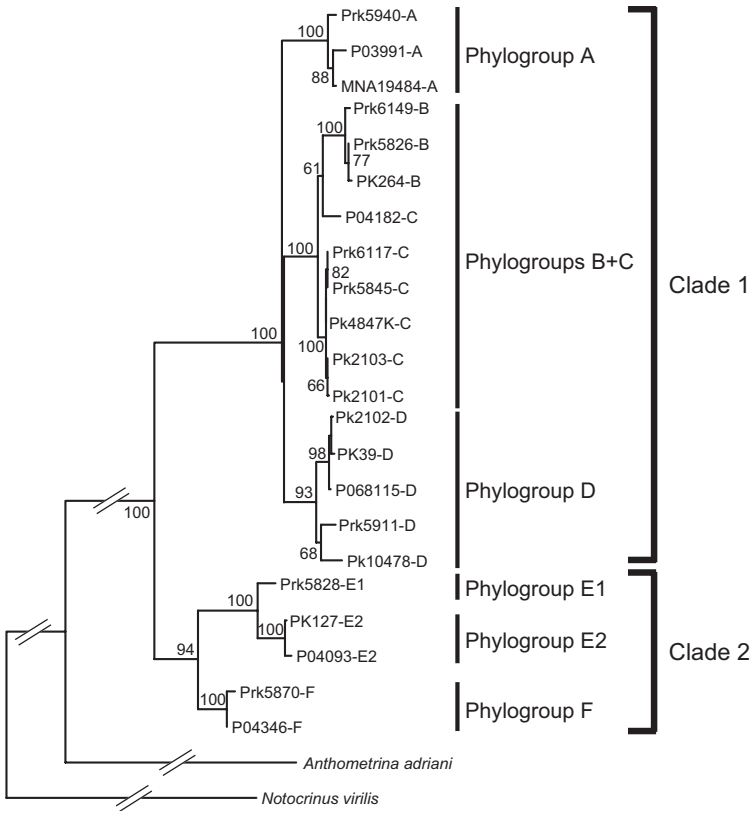

Fig. 5 Maximum likelihood phylogram of the concatenated data set of cytochrome c oxidase subunit I, Cytb, 16S, ITS and 28S for *Promachocrinus kerguelensis*. Values above branches are bootstraps.

The number of pairs of arms was found differentially distributed across the full COI haplotype network (Fig. 2). *Promachocrinus kerguelensis* usually display 10 pairs of arms, with variation ranging from 6 to 12 pairs. Specimens showing only six pairs of arms (called the 'six-radialed' specimens) are represented by only eight closely related haplotypes in phylogroup D (enclosed by thick, dashed line).

Population diversity and gene flow within phylogroups

Within-group genetic diversity was highly variable among phylogroups (Table 4). Phylogroups A (n = 314), C (n = 447) and D (n = 235) were the most represented in the data set and showed a high number of haplotypes (Table 4), whereas phylogroups B, E1, E2 and F were the least represented (<170 individuals) and showed very few haplotypes (<10). Phylogroups A, C and D showed high diversity indices (Hd > 0.65 and $\pi > 0.0025$), whereas phylogroups B and F showed medium indices ($0.5 < \text{Hd} < 0.65$ and $0.001 < \pi < 0.0025$) and phylogroups E1 and E2 showed low indices (Hd < 0.5 and < π <0.001). Phylogroups A, C, D, E1 and E2 showed overall significant negative values of Fu's F_S (Table 4), whereas these statistics were not significant for phylogroups B and F.

Within phylogroups, genetic diversity estimators showed great variability (Table 4, Fig. 6). Within phylogroup A, every population except BI had medium to high diversity indices. Within phylogroup B, diversity indices were rather medium, even low. Within phylogroup C, diversity indices were high in most populations, medium in SSa and low in SO and RS. Within phylogroup D, diversity indices were high in most population, medium in DS, DDU and WAP, and low in EWS2. Only one population (SO) of phylogroup E1 showed more than one haplotype with low diversity indices. Within phylogroups E2 and F, every population except EWS1 had low diversity indices. Some populations showed a high proportion of private haplotypes, mostly associated with a high haplotype diversity (Table 4, Fig. 6): KP (16/20), DDU (6/9) and RS (9/15) in phylogroup A; EWS1 (11/16), SSa (6/9) and DDU (9/14) in phylogroup C; SSh (7/10) and RS (7/12) in phylogroup D; SO (6/7) in phylogroup E1; and DDU (3/4) in phylogroup E2. Only some populations within every phylogroup displayed significant negative values of Fu's F_S (Table 4) that were correlated with unimodal

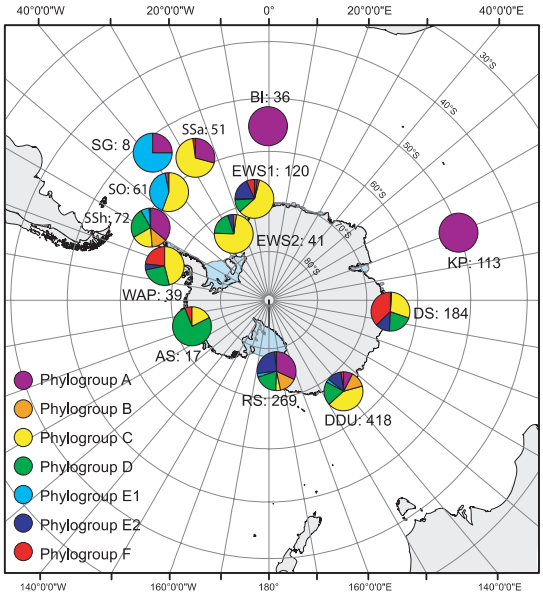

Fig. 6 Map showing the frequency of occurrence of each cytochrome c oxidase subunit I phylogroup of *Promachocrinus kerguelensis*. BI, Bouvet Island, EWS1, Kapp Norvegia, EWS2, Halley Bay, KP, Kerguelen Plateau, DS, Davis Sea, DDU, Dumont d'Urville Sea, RS, Ross Sea, AS, Amundsen Sea, WAP, West Antarctic Peninsula, SSh, South Shetland Islands, SO, South Orkney Islands, SSa, South Sandwich Islands, SG, South Georgia; numbers, sequenced specimens per region.

mismatch distribution (Fig. S2, Supporting information). Other populations were associated with uni-, bi- or multimodal mismatch distributions.

The F_{ST} and Φ_{ST} results were similar and indicated differences in gene flow among phylogroups (Table 5). Within phylogroup A, a lack of gene flow was inferred between every population except SSa and SSh. Within phylogroup B, a lack of gene flow was inferred between SSh and DDU. Within phylogroup C, a lack of gene flow was inferred between every population except between SSh, WAP, and EWS1, EWS2, DDU, DS individually. A lack of gene flow was inferred within phylogroup D for populations DS, DDU and RS, to their neighbouring populations, and between EWS2 and all other populations. Within phylogroup E1, gene flow was inferred among all populations. Patterns within phylogroup E2 were similar to E1, except that a lack of gene flow was inferred between EWS1 and all other populations. Within phylogroup F, a lack of gene flow was inferred between EWS1 and WAP, DDU, and between DS and WAP, DDU.

Discussion

Very few studies to date have used the scope of sampling necessary to assess whether benthic Antarctic invertebrates are truly circumpolar. Most are restricted by the logistical challenges that occur when sampling such a vast and remote ecosystem. Notable recent exceptions are seen in studies that have recovered evidence for a circum-Antarctic distribution for their target species: a single genetically homogenous distribution (Raupach *et al.* 2010) or a series of regionally isolated populations (Arango *et al.* 2011). In other studies that showed similar widespread sampling, one or more morphologically defined species showed an unexpected pattern of genetic diversity that did not correlate with the morphological species concept (Allcock *et al.* 2011; Baird *et al.* 2011), with at least one or more of these cryptic species showing potential for a circum-Antarctic distribution.

A complex of several sympatric, eurybathic and circumpolar lineages

The expansion of the sampling effort for *Promachocrinus kerguelensis* herein confirms and expands the findings of Wilson *et al.* (2007), in which several phylogroups were found to exist in sympatry. Whether these phylogroups can be interpreted as cryptic species is beyond the scope of this study. However, tentatively applying the criteria suggested by Held (2003) and Hart *et al.* (2006) to the present data set would support the existence of as few as two and as many as seven cryptic species. The two pairs of phylogroups B–C and E1–E2 show the lowest p-distances values observed here; however, a clear barcode-gap exists within E1–E2 (Fig. 4), lending support for two distinct lineages. All of the other pairwise distances fall into the range of those for other comatulid species: 3–6% in southern Australian and Indo-Pacific comatulids (Helgen & Rouse 2006; Owen *et al.* 2009). The phylogenetic tree yields good support for Clades 1 and 2 and for each phylogroup except phylogroup C. The status of phylogroup B is difficult to clarify, but because of the number of steps between these groups in the haplotype network, we chose to treat phylogroup B as a distinct mitochondrial entity. All these reasons lead us to consider that *P. kerguelensis* comprises seven mitochondrial phylogroups that appear to have undergone different demographic histories. However, the nuclear networks are more conservative and support the separation of two lineages, not seven (Fig. 3). These two nuclear lineages are consistent with Clades 1 and 2 retrieved using phylogenetic tools. Compared to the number of mutational steps between COI lineages within each clade (an average of nine steps within clade ABCD, 10 steps within clade EF), the number of differences between Clades 1 and 2 (19 steps in ITS + 28S, >60 steps in COI + Cytb) seems to be correlated with an interspecific rather than to an intraspecific

Table 4 Genetic diversity indices in each phylogroup and population from each phylogroup of *Promachocrinus kerguelensis*

	N	h	Hp	Hd	π	θ_π	θ_S	Fu's F_S
A								
DDU	32	9	6	0.6855	0.0043	2.3629	2.9797	−1.397
RS	86	15	9	0.6621	0.0048	2.6071	2.3877	−3.256
SSh	26	5	2	0.6092	0.0040	2.1631	2.3585	1.349
SSa	15	6	3	0.7619	0.0018	0.9905	1.5377	−2.841 **
BI	36	3	2	0.1619	0.0002	0.1111	0.4823	−2.590 ***
KP	113	20	16	0.7162	0.0019	1.0341	3.7735	−18.519 ***
Total	314	48	—	0.7816	0.0043	2.3441	6.6403	−26.584 ***
B								
DDU	54	8	4	0.6988	0.0017	0.9224	1.3167	−3.221 *
RS	40	5	1	0.5859	0.0015	0.7974	0.9404	−0.935
SSh	9	2	0	0.2222	0.0004	0.2222	0.3679	−0.263
Total	107	9	—	0.6410	0.0016	0.8436	1.1429	−3.691
C								
DS	54	5	2	0.6108	0.0013	0.7072	0.6583	−0.987
DDU	179	14	9	0.7423	0.0040	2.1795	2.7769	−2.056
RS	10	3	0	0.3778	0.0020	1.1111	1.4139	0.683
WAP	18	8	4	0.8301	0.0040	2.1699	4.0703	−2.202
SSh	13	5	2	0.6923	0.0016	0.8974	0.9667	−2.036 *
SO	34	4	1	0.4688	0.0010	0.5437	0.7337	−0.920
SSa	35	9	6	0.5664	0.0013	0.7193	1.9426	−6.758 ***
EWS2	30	5	0	0.6644	0.0027	1.4828	2.2718	0.430
EWS1	71	16	11	0.8072	0.0059	3.2177	3.9314	−3.258
Total	447	42	—	0.7300	0.0036	1.9533	5.3903	−26.788 ***
D								
DS	38	7	2	0.6088	0.0031	1.6657	2.6181	−0.660
DDU	82	12	5	0.6197	0.0044	2.3692	3.0134	−1.706
RS	53	12	7	0.8694	0.0074	4.0247	3.0850	−0.261
AS	13	4	2	0.7308	0.0029	1.5897	2.5780	0.514
WAP	10	4	1	0.5333	0.0047	2.5778	3.5349	1.176
SSh	18	10	7	0.8497	0.0083	4.5163	5.2332	−1.623
EWS1	13	8	3	0.8590	0.0054	2.9359	3.8670	−2.291
EWS2	8	3	0	0.4643	0.0035	1.9286	2.6997	1.493
Total	235	36	—	0.8512	0.0067	3.6500	5.7998	−15.310 ***
E1								
DDU	11	1	0	0.0000	0.0000	0.0000	0.0000	—
RS	8	1	0	0.0000	0.0000	0.0000	0.0000	—
SSh	5	1	0	0.0000	0.0000	0.0000	0.0000	—
SO	25	7	6	0.4300	0.0012	1.8538	0.6333	−4.900 ***
SG	6	1	0	0.0000	0.0000	0.0000	0.0000	—
Total	56	7	—	0.2045	0.0005	0.2844	1.5238	−7.141 ***
E2								
DS	22	1	0	0.0000	0.0000	0.0000	0.0000	—
DDU	51	4	3	0.1153	0.0002	0.1176	0.6668	−4.339 ***
RS	68	2	1	0.0294	0.0001	0.0294	0.2088	−1.894 ***
EWS1	22	4	2	0.7056	0.0016	0.8874	0.5486	−0.184
Total	167	8	—	0.2016	0.0004	0.2301	1.0541	−8.688 ***
F								
DS	68	3	1	0.5083	0.0009	0.5088	0.4176	0.580
DDU	9	1	0	0.0000	0.0000	0.0000	0.0000	—
WAP	9	1	0	0.0000	0.0000	0.0000	0.0000	—
EWS1	8	3	1	0.6071	0.0014	0.7857	0.7713	−0.224
Total	103	4	—	0.4574	0.0008	0.4637	0.5761	−0.558

N, number of sequences; h, number of haplotypes; Hp, number of private haplotypes; Hd, haplotypic diversity; π, nucleotide diversity; θ_π, average number of nucleotide differences; θ_S, average number of polymorphic sites; BI, Bouvet Island; EWS1, Kapp Norvegia; EWS2, Halley Bay; KP, Kerguelen Plateau; DS, Davis Sea; DDU, Dumont d'Urville Sea; RS, Ross Sea; AS, Amundsen Sea; WAP, West Antarctic Peninsula; SSh, South Shetland Islands; SO, South Orkney Islands; SSa, South Sandwich Islands; SG, South Georgia.
Significance of Fu's F_S is represented with asterisk: *$P < 0.05$; **$P < 0.01$; ***$P < 0.005$.

Table 5 Pairwise F_{ST} values (below diagonal) and Φ_{ST} (above diagonal) between populations in each phylogroup of *Promachocrinus kerguelensis*

A	KP	BI	SSh	SSa	DDU	RS
KP		**0.1198**	**0.2402**	**0.1307**	**0.5786**	**0.4752**
BI	**0.1202**		**0.2214**	**0.1321**	**0.5923**	**0.4317**
SSh	**0.2392**	**0.2220**		0.0928	**0.1936**	**0.1521**
SSa	**0.1306**	**0.1329**	0.0927		**0.4280**	**0.3217**
DDU	**0.5770**	**0.5922**	**0.1931**	**0.4273**		**0.0290**
RS	**0.4747**	**0.4325**	**0.1524**	**0.3129**	**0.0289**	

C	SSa	SO	EWS1	EWS2	SSh	WAP	RS	DDU	DS
SSa		**0.0402**	**0.1592**	**0.1864**	**0.3499**	**0.1202**	**0.5955**	**0.1483**	**0.2151**
SO	**0.0401**		**0.1161**	**0.0879**	**0.2467**	**0.0436**	**0.5854**	**0.0840**	**0.0837**
EWS1	**0.1587**	**0.1162**		**0.0493**	0.0608	0.0443	**0.1982**	**0.0644**	**0.1029**
EWS2	**0.1860**	**0.0877**	**0.0496**		−0.0127	−0.0198	**0.2868**	−0.0077	0.0062
SSh	**0.3495**	**0.2466**	0.0614	−0.0123		0.0116	**0.3310**	0.0017	0.0401
WAP	**0.1201**	0.0440	0.0442	−0.0196	0.0124		**0.2741**	0.0096	0.0209
RS	**0.5954**	**0.5856**	**0.1987**	**0.2878**	**0.3316**	**0.2753**		**0.1736**	**0.4495**
DDU	**0.1482**	**0.0841**	**0.0645**	−0.0076	0.0022	0.0098	**0.1743**		**0.0374**
DS	**0.2148**	**0.0867**	**0.1032**	0.0060	0.0400	0.0212	**0.4498**	**0.0375**	

D	EWS1	EWS2	SSh	WAP	AS	RS	DDU	DS
EWS1		0.1107	0.0073	0.0263	0.0589	**0.0736**	**0.3200**	**0.5070**
EWS2	**0.1113**		**0.1451**	**0.2833**	**0.3294**	**0.2010**	**0.4518**	**0.6298**
SSh	0.0077	**0.1458**		0.0084	0.0519	**0.1004**	**0.3853**	**0.5043**
WAP	0.0270	**0.2848**	0.0093		−0.0454	**0.1516**	**0.4445**	**0.6178**
AS	0.0511	**0.3303**	0.0527	−0.0453		**0.1929**	**0.4854**	**0.6673**
RS	**0.0739**	**0.2015**	**0.1009**	**0.1522**	**0.1931**		**0.2051**	**0.2974**
DDU	**0.3196**	**0.4518**	**0.3851**	**0.4445**	**0.4850**	**0.2054**		**0.0470**
DS	**0.5063**	**0.6294**	**0.5043**	**0.6176**	**0.6667**	**0.2975**	**0.0468**	

E1	SG	SO	SSh	RS	DDU
SG		−0.0788	0.0000	0.0000	0.0000
SO	−0.0785		−0.0998	−0.0527	−0.0308
SSh	0.0000	−0.0995		0.0000	0.0000
RS	0.0000	−0.0525	0.0000		0.0000
DDU	0.0000	−0.0306	0.0000	0.0000	

B	SSh	RS	DDU
SSh		0.0980	**0.1616**
RS	0.0980		0.0030
DDU	**0.1616**	0.0030	

E2	EWS1	RS	DDU	DS
EWS1		**0.5176**	**0.4182**	**0.3490**
RS	**0.5178**		0.0032	−0.0208
DDU	**0.4182**	0.0032		−0.0190
DS	**0.3492**	−0.0208	−0.0190	

F	EWS1	WAP	DS	DDU
EWS1		**0.4973**	0.0651	**0.4973**
WAP	**0.4975**		**0.2059**	0.0000
DS	0.0653	**0.2059**		**0.2059**
DDU	**0.4975**	0.0000	**0.2059**	

AS, Amundsen Sea; BI, Bouvet Island; DDU, Dumont d'Urville Sea; DS, Davis Sea; KP, Kerguelen Plateau; RS, Ross Sea; SG, South Georgia; SO, South Orkney Islands; SSa, South Sandwich Islands; SSh, South Shetland Islands; WAP, West Antarctic Peninsula. Of 1023 permutations, significant values ($P < 0.05$) are in bold, and names of populations are given in Table 4.

divergence. Moreover, there is a perfect individual assignation between mitochondrial and nuclear haplotypes, suggesting that hybridization does not occur between these two clades. All of these results together suggest that Clades 1 and 2 can be interpreted as putative cryptic species and that the species name *Promachocrinus kerguelensis* should be reserved to Clade 1, as it is the only one recovered from the vicinity of the type locality at the KP.

All mitochondrial phylogroups appeared eurybathic and were found living in sympatry. However, even if all the phylogroups are widespread on the Antarctic

continental shelf, several phylogroups are absent from many Sub-Antarctic regions (Fig. 6). Phylogroup E2 is absent from SSh; phylogroups B, D and E2 are absent from SO; only phylogroups A, C and F are found in SSa; specimens from SG are members of phylogroups A and E1. Phylogroup A is the only one present on BI and KP. These different distributions could be the result of populations isolated in different refugia during past

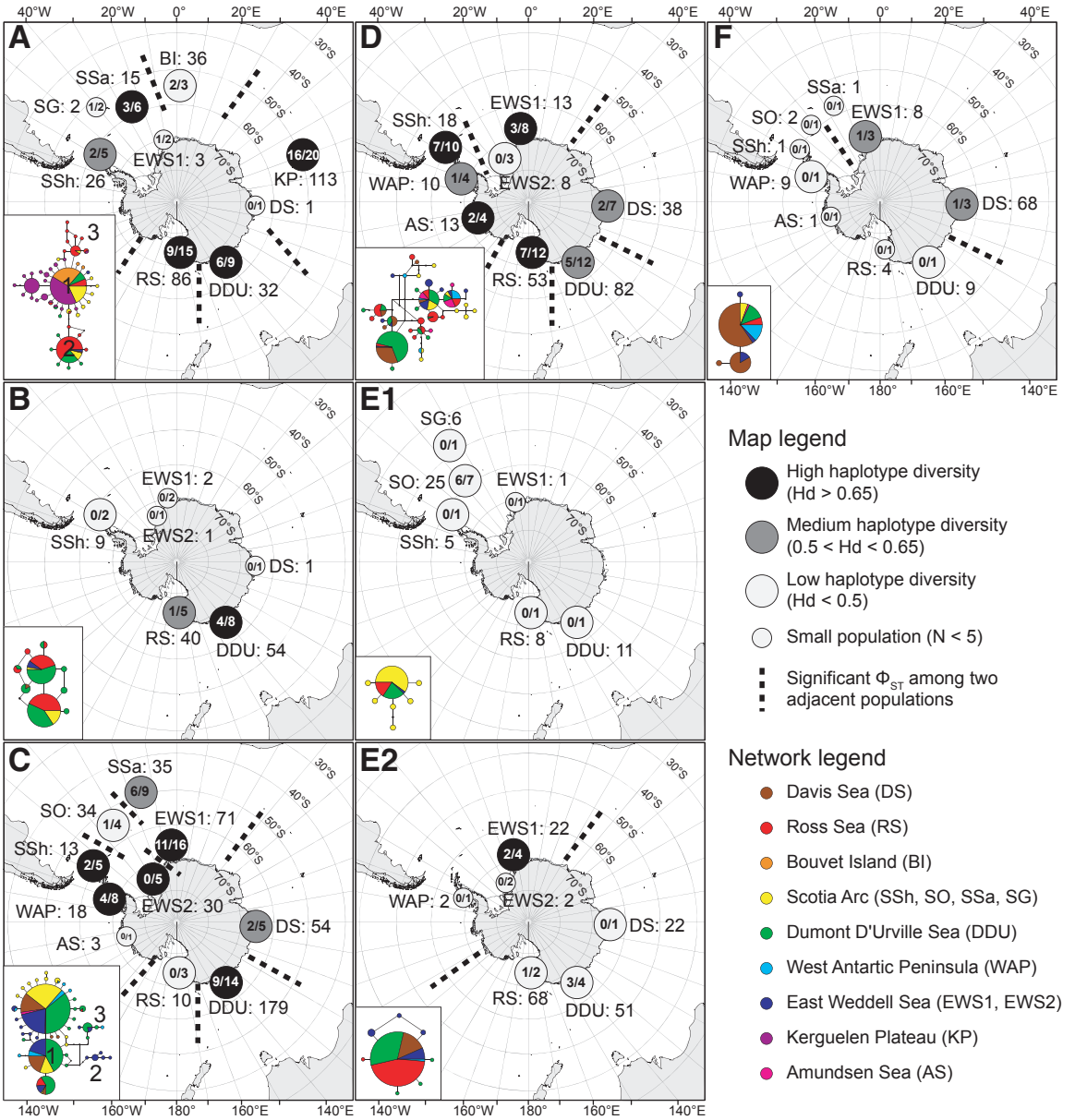

Fig. 7 Diversity, haplotype distribution and connectivity maps for the seven cytochrome c oxidase subunit I (COI) phylogroups A, B, C, D, E1, E2 and F of *Promachocrinus kerguelensis*. Filled circles, haplotype diversity (Hd) per population; numbers inside circles, proportion of private haplotypes to total number of haplotypes; dashed lines, barrier to gene flow between adjacent populations; BI, Bouvet Island; EWS1, Kapp Norvegia; EWS2, Halley Bay; KP, Kerguelen Plateau; DS, Davis Sea; DDU, Dumont d'Urville Sea; RS, Ross Sea; AS, Amundsen Sea; WAP, West Antarctic Peninsula; SSh, South Shetland Islands; SO, South Orkney Islands; SSa, South Sandwich Islands; SG, South Georgia; numbers, sequenced specimens per population; boxes are the COI haplotype networks.

glacial events, followed by dispersal, colonization and secondary contact during interglacial periods. The differing divergences among phylogroups (five mutational steps in COI between E1–E2, and up to 22 between D–F) are likely to be the result of different glaciation events predating the Last Glacial Maximum (LGM; ~18–20 kya BP).

Contrasting population history among phylogroups

Comparisons of intragroup genetic diversity, haplotype network structures, inferences of gene flow and demographic indices reveal that the seven phylogroups in *Promachocrinus* do not share the same population history. Phylogroups A, C and D show lots of highly diverse populations, some of them with a high proportion of private haplotypes (Fig. 7). Most of these populations could be considered as distinct refugial populations within their respective phylogroups, or populations resulting from secondary contact after migration events from several source populations (Maggs *et al.* 2008). Unlike the nemertean *Parborlasia corrugatus* (Thornhill *et al.* 2008) and the ophiurid *Astrotoma agassizii* (Hunter & Halanych 2008), the genetic diversity within these three phylogroups of *P. kerguelensis* does not decrease with increasing latitude. During the LGM, grounded ice sheets are thought to have extended across nearly the whole Antarctic continental shelf, dramatically impacting the benthic communities. Some areas might have been left free of ice, acting as refugia (Thatje *et al.* 2005, 2008). Of all the phylogroups, only A, C and D have multiple sampled localities with high haplotypic diversity. Of these, phylogroup A also has a high number of private haplotypes and high proportion of the ancestral haplotype (haplotype 1 in network inset in Fig. 7A) at KP, which is congruent with a glacial refugium situated on the KP. The same seems true for the RS + DDU populations, which show a high number of private haplotypes and a high proportion of a haplotype shared only between truly Antarctic populations (haplotype 2 in Fig. 7A), indicating a second refugium in the RS area. The presence of another group of haplotypes (haplotype 3 in Fig. 7A) from the RS closely related to the ancestral haplotype is indicative of a polyphyletic genealogy because of an incomplete lineage sorting in this population during the LGM. For phylogroup C, multiple refugia may be inferred at Kapp Norvegia (Weddell Sea), (haplotypes 1 and 2, Fig. 7C) and at DDU. The structure of the phylogroup D is very complex and does not appear to display a clear signal. Populations from the Peninsula and the Scotia Arc of the phylogroups A and C show evidences of secondary contact owing to past migrations from source populations in different refugia. However, this still has to be tested by using other genetic loci. In contrast, only one or two populations within phylogroups B, E1, E2 and F show high to moderate levels of genetic diversity, and most populations within these phylogroups show a much-reduced diversity indicating a prolonged and/or severe bottleneck. For phylogroup E1, the SO population is the most diversified and seems to be an indicative of a refugium even if it also shows a signal of a strong bottleneck. Subsequent widespread dispersal from these refugial populations is possible as a consequence of larval transport by the clockwise ACC and the weaker counter clockwise Antarctic Coastal Current (CC). Population history of these different phylogroups of *P. kerguelensis* suggests that they underwent strong demographic events that severely impacted their genetic diversity on the continental shelf. Those events are most likely to be the result of a long history of glaciations in Antarctica (Zachos *et al.* 2001) with the persistence of some populations from different phylogroups in a few refugia on the continental shelf, namely: the DDU, the RS, Kapp Norvegia in the Weddell Sea, in the Scotia Arc around the South Shetland and SO, and on the KP in the Sub-Antarctic region.

Regional patterns of gene flow

At the tip of the Antarctic Peninsula and along the Scotia Arc, strong signals of connectivity can be found, and only phylogroup C shows a lack of gene flow between neighbouring populations (Fig. 7). This interestingly contrasts with recent suggestions that the Scotia Arc is a centre of diversification for marine benthic taxa (Linse *et al.* 2007; Griffiths *et al.* 2008; Allcock *et al.* 2011), with allopatry attributed to complex geography and bathymetry. The absence of barrier to gene flow observed among *P. kerguelensis* populations at the tip of the Antarctic Peninsula and the Scotia Arc is probably a result of the strong current system that surrounds this area. While the Antarctic Slope Front (ASF) and the Weddell Front (WF) flow northward from the eastern side of the Antarctic Peninsula, the Antarctic CC flows in and out the Bransfield Strait along the western side of the peninsula (Thompson *et al.* 2009), connecting the populations SSh and WAP. The ASF and CC come into confluence with the ACC around the South Scotia Ridge, becoming the Weddell Scotia Confluence and forming a high number of eddies northeast of Clarence Island, mixing waters and dispersing larvae therein (Patterson & Sievers 1980; Thompson *et al.* 2009). This current system could act as a vector of migration from different source populations elsewhere in the Southern Ocean, leading to a strong contact zone between several populations in this region.

The two Sub-Antarctic regions examined in this study are notable for their lack of diversity. Only phylogroup A was represented at both the KP and BI, although no

evidence for gene flow between the two could be inferred (Fig. 7). Recent colonization of the Sub-Antarctic islands has been suggested for kelps (Fraser *et al.* 2009) and crustaceans (Nikula *et al.* 2010), attributed to ice sheet retreat after the LGM. This seems likely for phylogroup A on the young and isolated volcanic BI (Arntz *et al.* 2006), which was genetically depauperate. However, the population on the KP is thought to be the result of *in situ* diversification within a glacial refugium, at least during the LGM. The KP is directly in the path of the ACC, and this area could also potentially receive migrants from several western populations not sampled in this study (e.g. Crozet Islands). The addition of nuclear markers may help to distinguish *in situ* diversification from diversity received by migration.

Another important result highlighted by Φ_{ST} is the poor degree of connectivity between populations on the east Antarctic continental shelf. A significant break in gene flow occurs between DDU and Davis Sea for all but one of the *Promachocrinus* phylogroups. Additionally, although RS and DDU populations appear highly connected for three *Promachocrinus* phylogroups, there is also evidence of restricted intraspecific gene flow within three other phylogroups (A, C and D). This pattern is also present in data from Baird *et al.* (2011), where at least two of their cryptic species clades showed significant breaks between two East Antarctic locations. Moreover, while the species examined in Baird *et al.* (2011) are brooders, and might be expected to show such structure, *P. kerguelensis* is thought to be a broadcast spawner, with lecithotrophic larvae (McClintock & Pearse 1987). It appears that the East Antarctic coast may host significant barriers to gene flow, affecting multiple taxa with varying reproductive strategies.

Conclusions

The comprehensive sampling used here with respect to geographical scale and number of specimens is unprecedented in Antarctic benthic studies. Our increased sampling of *Promachocrinus kerguelensis* corroborated the six phylogroups identified in Wilson *et al.* (2007). Moreover, we discovered an additional phylogroup (E2). These seven phylogroups belong to two well-supported clades that are sympatric, eurybathic and circumpolar. These could represent two cryptic species within the widespread feather star *P. kerguelensis*. Glacial refugia linked to the LGM are well documented in the North Atlantic (Maggs *et al.* 2008 and references therein). In the Southern Ocean, glacial refugia are thought to have been the source for recolonization of the Antarctic continental shelf, but until now this hypothesis was never carefully documented. Here, we show that some of the seven phylogroups of *P. kerguelensis* may serve as an evidence for glacial refugia on the KP, in the RS—Dumont d'Urville area, in the Bransfield Strait—South Shetland area and in the Eastern Weddell Sea area. These results compared to those of other widespread Antarctic benthic species will help understand the tempo of diversification and migration that led to the observed biodiversity in the Southern Ocean.

Acknowledgements

We first would like to acknowledge people without whom this huge amount of crinoids would not be gathered: Ty Hibberd (AAD, Hobart), Owen Anderson, David Bowden, Sadie Mills, Kareen Schnabel and Peter Smith (NIWA, Wellington), Stefano Schiaparelli (University of Genoa), Jens Bohn and Eva Lodde (ZSM, Munich), David Barnes, Katrin Linse, Huw Griffiths and Chester Sands (BAS, Cambridge). We thank also the CEAMARC (IPY project 53), POKERII and AMLR2009 cruises. We thank the ANTFLOCKS project funded by the French national research agency ('ANR'; USAR no 07-BLAN-0213-01). Funding parties also include the Département des Milieux et Peuplements Aquatiques at the Muséum national d'Histoire naturelle (MNHN) in Paris; three Actions Transversales du MNHN: 'Biodiversité actuelle et fossile; crises, stress, restaurations et panchronisme: le message systématique', 'Taxonomie moléculaire: DNA Barcode et gestion durable des collections' and 'Biominéralisation'; the French Polar Institute IPEV (travel grants to LGH and ME on REVOLTA); the NSF Antarctic Organisms and Ecosystems grant ANT-1043749 and the Antarctic Science Career Development Bursary (to NGW). This work was supported by the Consortium National de Recherche en Génomique, and the Service de Systématique Moléculaire (SSM) at the MNHN (USM 2700). It is part of the agreement number 2005/67 between the Génoscope and the MNHN on the project 'Macrophylogeny of life' directed by Guillaume Lecointre. Part of the molecular work was also supported by collaboration between the Census of Antarctic Marine Life, the Marine Barcode of Life (MarBOL) project and the Canadian Centre for DNA Barcoding (CCDB). Part of the material from the Ross Sea has been made available by the Italian PNRA Project 'BAMBi' (2010/A1.10) directed by Stefano Schiaparelli. DS was supported by funding of the Alfred P. Sloan Foundation to MarBOL. Laboratory analyses on sequences generated at the CCDB were funded by the Government of Canada through Genome Canada and the Ontario Genomics Institute (2008-OGI-ICI-03). Finally, we gratefully thank Lucile Perrier, Charlotte Tarin, Jose Ignacio Carvajal III Patterson (students) and Céline Bonillo (SSM) for their invaluable help in the molecular laboratory. We also gratefully thank Christoph Held (AWI), the two anonymous referees and Stephen Palumbi for their constructive comments that helped to improve the manuscript.

References

Allcock AL, Barratt I, Eléaume M *et al.* (2011) Cryptic speciation and the circumpolarity debate: a case study on endemic Southern Ocean octopuses using the COI barcode of life. *Deep-Sea Research Part II-Topical Studies in Oceanography*, **58**, 242–249.

Arango CP, Soler-Membrives A, Miller KJ (2011) Genetic differentiation in the circum-Antarctic sea spider *Nymphon australe* (Pycnogonida; Nymphonidae). *Deep-Sea Research Part II-Topical Studies in Oceanography*, **58**, 212–219.

Arntz WE, Thatje S, Linse K *et al.* (2006) Missing link in the Southern Ocean: sampling the marine benthic fauna of remote Bouvet Island. *Polar Biology*, **29**, 83–96.

Baird HP, Miller KJ, Stark JS (2011) Evidence of hidden biodiversity, ongoing speciation and diverse patterns of genetic structure in giant Antarctic amphipods. *Molecular Ecology*, **20**, 3439–3454.

Bell FJ (1908) Echinoderma. In: *National Antarctic Expedition* 1901–1904 (eds Bell FJ and Fletcher L) Natural History, Zoology (various invertebrata), **4**, 1–5.

Brandao SN, Sauer J, Schon I (2010) Circumantarctic distribution in Southern Ocean benthos? A genetic test using the genus Macroscapha (Crustacea, Ostracoda) as a model. *Molecular Phylogenetics and Evolution*, **55**, 1055–1069.

Carpenter PH (1888) Report on the Crinoidea collected during the voyage of H.M.S. Challenger, during the years 1873–76, Part II – The Comatulae. Report on the Scientific Results of the Voyage of H.M.S. Challenger, Zoology, London **26**, 1–399.

Clark AH, Clark AM (1967) A monograph of the existing crinoids. Volume 1 – The comatulids. Part 5 – Suborders Oligophreata (concluded) and Macrophreata. *Bulletin of the United States National Museum*, **82**, 1–795.

Clarke A, Crame JA (1992) The Southern Ocean benthic fauna and climate change: a historical perspective. *Philosophical Transactions of the Royal Society of London, Series B: Biological Sciences*, **338**, 299–309.

Clarke A, Crame JA (2010) Evolutionary dynamics at high latitudes: speciation and extinction in polar marine faunas. *Philosophical Transactions of the Royal Society of London, Series B: Biological Sciences*, **365**, 3655–3666.

Clement M, Posada D, Crandall KA (2000) TCS: a computer program to estimate gene genealogies. *Molecular Ecology*, **9**, 1657–1659.

Cohen BL, Améziane N, Eléaume M, Richer de Forges B (2004) Crinoid phylogeny: a preliminary analysis (Echinodermata: Crinoidea). *Marine Biology*, **144**, 605–617.

Eléaume M (2006) *Approche morphométrique de la variabilité phénotypique : consequences systématiques et évolutives. Application aux crinoïdes actuels (Crinoidea: Echinodermata).* PhD Dissertation, Muséum National d'Histoire Naturelle, Paris 1–402.

Eléaume M, Hemery LG, Bowden DA, Roux M (2011) A large new species of the genus *Ptilocrinus* (Echinodermata, Crinoidea, Hyocrinidae) from Antarctic seamounts. *Polar Biology*, **34**, 1385–1397.

Excoffier L, Lischer HEL (2010) Arlequin suite ver 3.5: a new series of programs to perform population genetics analyses under Linux and Windows. *Molecular Ecology Resources*, **10**, 564–567.

Folmer O, Black M, Hoeh W, Lutz R, Vrijenhoek R (1994) DNA primers for amplification of mitochondrial cytochrome *c* oxidase subunit I from diverse metazoan invertebrates. *Molecular Marine Biology and Biotechnology*, **3**, 294–299.

Fraser CI, Nikula R, Spencer HG, Waters JM (2009) Kelp genes reveal effects of subantarctic sea ice during the Last Glacial Maximum. *Proceedings of the National Academy of Sciences of the United States of America*, **106**, 3249–3253.

Griffiths HJ, Linse K, Barnes DKA (2008) Distribution of macrobenthic taxa across the Scotia Arc, Southern Ocean. *Antarctic Science*, **20**, 213–226.

Hall TA (1999) BioEdit: a user-friendly biological sequence alignment editor and analysis program for Windows 95/98/NT. *Nucleic Acids Symposium Series*, **41**, 95–98.

Hart MW, Keever CC, Dartnall AJ, Byrne M (2006) Morphological and genetic variation indicate cryptic species within Lamarck's little sea star, *Parvulastra* (=*Patiriella*) *exigua*. *Biological Bulletin*, **210**, 158–167.

Havermans C, Nagy ZT, Sonet G, De Broyer C, Martin P (2011) DNA barcoding reveals new insights into the diversity of Antarctic species of *Orchomene sensu lato* (Crustacea: Amphipoda: Lysianassoidea). *Deep-Sea Research Part II-Topical Studies in Oceanography*, **58**, 230–241.

Heimeier D, Lavery S, Sewell MA (2010) Molecular species identification of *Astrotoma agassizii* from planktonic embryos: Further evidence for a cryptic species complex. *Journal of Heredity*, **101**, 775–779.

Held C (2003) Molecular evidence for cryptic speciation within the widespread Antarctic crustacean *Ceratoserolis trilobitoides* (Crustacea, Isopoda). In: *Antarctic Biology in a Global Context* (eds Huiskes AHL, Giekes WWC, Rozema J, Schorno RML *et al.*), pp. 135–139. Backhuys Publisher, Leiden, The Netherlands.

Held C, Wagele JW (2005) Cryptic speciation in the giant Antarctic isopod *Glyptonotus antarcticus* (Isopoda: Valvifera: Chaetiliidae). *Scientia Marina*, **69**, 175–181.

Helgen LE, Rouse GW (2006) Species delimitation and distribution in *Aporometra* (Crinoidea: Echinodermata): endemic Australian featherstars. *Invertebrate Systematics*, **20**, 395–414.

Hunter RL, Halanych KM (2008) Evaluating connectivity in the brooding brittle star *Astrotoma agassizii* across the Drake passage in the Southern Ocean. *Journal of Heredity*, **99**, 137–148.

Hunter RL, Halanych KM (2010) Phylogeography of the Antarctic planktotrophic brittle star *Ophionotus victoriae* reveals genetic structure inconsistent with early life history. *Marine Biology*, **157**, 1693–1704.

Ivanova NV, Dewaard JR, Hebert PD (2006) An inexpensive, automation-friendly protocol for recovering high-quality DNA. *Molecular Ecology Notes*, **6**, 998–1002.

Jobb G (2008) TREEFINDER version of October 2008. Munich, Germany. Distributed by the author at http://www.treefinder.de.

Knowlton N (1993) Sibling species in the sea. *Annual Review of Ecology and Systematics*, **24**, 189–216.

Knowlton N (2000) Molecular genetic analyses of species boundaries in the sea. *Hydrobiologia*, **420**, 73–90.

Krabbe K, Leese F, Mayer C, Tollrian R, Held C (2010) Cryptic mitochondrial lineages in the widespread pycnogonid *Colossendeis megalonyx* Hoek, 1881 from Antarctic and Subantarctic waters. *Polar Biology*, **33**, 281–292.

Leese F, Held C (2008) Identification and characterization of microsatellites from the Antarctic isopod *Ceratoserolis trilobitoides*: nuclear evidence for cryptic species. *Conservation Genetics*, **9**, 1369–1372.

Librado P, Rozas J (2009) DnaSP v5: a software for comprehensive analysis of DNA polymorphism data. *Bioinformatics*, **25**, 1451–1452.

Linse K, Cope T, Lorz AN, Sands C (2007) Is the Scotia Sea a centre of Antarctic marine diversification? Some evidence of cryptic speciation in the circum-Antarctic bivalve Lissarca notorcadensis (Arcoidea : Philobryidae). *Polar Biology*, **30**, 1059–1068.

Maggs CA, Castilho R, Foltz D *et al.* (2008) Evaluating signatures of glacial refugia for North Atlantic benthic marine taxa. *Ecology*, **89**, S108–S122.

Marr JWS (1963) Unstalked crinoids of Antarctic continental shelf – notes on their natural history and distribution. *Philosophical Transactions of the Royal Society of London Series B-Biological Sciences*, **246**, 327–379.

McClintock JB, Pearse JS (1987) Reproductive biology of the common Antarctic crinoid *Promachocrinus kerguelensis* (Echinodermata, Crinoidea). *Marine Biology*, **96**, 375–383.

Meyer CP, Paulay G (2005) DNA barcoding: error rates based on comprehensive sampling. *PLoS Biology*, **3**, e422.

Mortensen T (1917) *Notocrinus virilis* n. g., n. sp. a new viviparous crinoid from the Antarctic Sea. *Videnskabelige Meddelelser Naturhistorisk Forening i København*, **68**, 205–208.

Nikula R, Fraser CI, Spencer HG, Waters JM (2010) Circumpolar dispersal by rafting in two subantarctic kelp-dwelling crustaceans. *Marine Ecology Progress Series*, **405**, 221–230.

Owen CL, Messing CG, Rouse GW, Shivji MS (2009) Using a combined approach to explain the morphological and ecological diversity in *Phanogenia gracilis* Hartlaub, 1893 (Echinodermata: Crinoidea) sensu lato: two species or intraspecific variation? *Marine Biology*, **156**, 1517–1529.

Patterson SL, Sievers HA (1980) The Weddell – Scotia confluence. *Journal of Physical Oceanography*, **10**, 1584–1610.

Posada D, Crandall KA (2001) Intraspecific gene genealogies: trees grafting into networks. *Trends in Ecology & Evolution*, **16**, 37–45.

Ratnasingham S, Hebert PDN (2007) BOLD: the barcode of life data system (http://www.barcodinglife.org). *Molecular Ecology Notes*, **7**, 355–364.

Raupach MJ, Wagele JW (2006) Distinguishing cryptic species in Antarctic Asellota (Crustacea: Isopoda) – a preliminary study of mitochondrial DNA in *Acanthaspidia drygalskii*. *Antarctic Science*, **18**, 191–198.

Raupach MJ, Malyutina M, Brandt A, Wagele JW (2007) Molecular data reveal a highly diverse species flock within the munnopsoid deep-sea isopod *Betamorpha fusiformis* (Barnard, 1920) (Crustacea: Isopoda: Asellota) in the Southern Ocean. *Deep-Sea Research Part II-Topical Studies in Oceanography*, **54**, 1820–1830.

Raupach MJ, Thatje S, Dambach J, Rehm P, Misof B, Leese F (2010) Genetic homogeneity and circum-Antarctic distribution of two benthic shrimp species of the Southern Ocean, *Chorismus antarcticus* and *Nematocarcinus lanceopes*. *Marine Biology*, **157**, 1783–1797.

Schüller M (2011) Evidence for a role of bathymetry and emergence in speciation in the genus *Glycera* (Glyceridae, Polychaeta) from the deep Eastern Weddell Sea. *Polar Biology*, **34**, 549–564.

Speel JA, Dearborn JH (1983) Comatulid crinoids from the R/V *Eltanin* cruises in the Southern Ocean. *Antarctic Research Series*, **38**, 1–60.

Tamura K (1992) Estimation of the number of nucleotide substitutions when there are strong transition-transversion and G+C content biases. *Molecular Biology and Evolution*, **9**, 678–687.

Tamura K, Peterson D, Peterson N, Stecher G, Nei M, Kumar S (2011) MEGA5: molecular evolutionary genetics analysis using maximum likelihood, evolutionary distance, and maximum parsimony methods. *Molecular Biology and Evolution*, **28**, 2731–2739.

Thatje S, Hillenbrand CD, Larter R (2005) On the origin of Antarctic marine benthic community structure. *Trends in Ecology & Evolution*, **20**, 534–540.

Thatje S, Hillenbrand CD, Mackensen A, Larter R (2008) Life hung by a thread: endurance of Antarctic fauna in glacial periods. *Ecology*, **89**, 682–692.

Thompson AF, Heywood KJ, Thorpe SE, Renner AHH, Trasvina A (2009) Surface circulation at the tip of the Antarctic Peninsula from drifters. *Journal of Physical Oceanography*, **39**, 3–26.

Thornhill DJ, Mahon AR, Norenburg JL, Halanych KM (2008) Open-ocean barriers to dispersal: a test case with the Antarctic Polar Front and the ribbon worm *Parborlasia corrugatus* (Nemertea: Lineidae). *Molecular Ecology*, **17**, 5104–5117.

Wilson NG, Hunter RL, Lockhart SJ, Halanych KM (2007) Multiple lineages and absence of panmixia in the ''circumpolar'' crinoid *Promachocrinus kerguelensis* from the Atlantic sector of Antarctica. *Marine Biology*, **152**, 895–904.

Wilson NG, Schrödl M, Halanych KM (2009) Ocean barriers and glaciation: evidence for explosive radiation of mitochondrial lineages in the Antarctic sea slug *Doris kerguelenensis* (Mollusca, Nudibranchia). *Molecular Ecology*, **18**, 965–984.

Zachos J, Pagani M, Sloan L, Thomas E, Billups K (2001) Trends, rhythms, and aberrations in global climate 65 Ma to present. *Science*, **292**, 686–693.

L.G.H. is a benthic biologist interested in marine invertebrates molecular evolution, population dynamics, habitat modelling and community ecology. M.E. is a crinoid taxonomist interested in marine invertebrates evolutionary history, biogeography, and ecology. V.R. is interested in population genetics of plant (cultivated, wild and invasive) and animal (fish and marine invertebrates), phylogeography of marine invertebrates, and quantitative genetics of plants and marine invertebrates. N.A. is a crinoid taxonomist interested in ontogenetic trends, phenotypic variation in relation to environmental constraints, biogeography and conservation biology. C.G. is a bioinformatician and evolutionary biologist who is interested in phylogeny and diversity of Antarctic organisms. D.S. is interested in molecular evolution of aquatic organisms and works on practical and theoretical aspects of DNA barcoding. N.G.W. is an evolutionary biologist who is interested in the phylogeography, phylogeny and diversity of marine organisms.

Data accessibility

All cytochrome c oxidase subunit I sequences have been deposited on BOLD in the project ≪ PROKE ≫. Details of all sampled locations and sequence Accession nos are provided in Supporting Information (Table S1, Supporting information). 16S, ITS, 28S and Cytb sequences are deposited on GenBank under the Accession nos JQ340210 to JQ340234, JQ340235 to JQ340259, JQ340260 to JQ340284 and JQ340285 to JQ340309, respectively.

Supporting information

Additional supporting information may be found in the online version of this article.

Table S1 Sampling location details, haplotype details and sequences Accession nos of all *Promachocrinus* specimens.

Fig. S1 Distribution maps for the seven phylogroups A, B, C, D, E1, E2 and F of the *P. kerguelensis* complex in the Southern Ocean.

Fig. S2 Observed and simulated mismatch distributions under models of demographic expansion and spatial expansion for each population of the seven phylogroups A, B, C, D, E1, E2 and F of the *P. kerguelensis* complex.

Please note: Wiley-Blackwell are not responsible for the content or functionality of any supporting information supplied by the authors. Any queries (other than missing material) should be directed to the corresponding author for the article.

Supporting information

Table S1. Sampling location details, haplotype details and sequences accession numbers of all *Promachocrinus* specimens.

Figure S1. Distribution maps for the seven phylogroups A, B, C, D, E1, E2 and F of the *P. kerguelensis* complex in the Southern Ocean. Circles = populations >5 specimens; squares = populations <5 specimens; BI = Bouvet Island, EWS1 = Kapp Norvegia, EWS2 = Halley Bay, KP = Kerguelen Plateau, DS = Davis Sea, DDU = Dumont d'Urville Sea, RS = Ross Sea, AS = Amundsen Sea, WAP = West Antarctic Peninsula, SSh = South Shetland Islands, SO = South Orkney Islands, SSa = South Sandwich Islands, SG = South Georgia; numbers = sequenced specimens per population.

Figure S2. Observed and simulated mismatch distributions under models of demographic expansion and spatial expansion for each population of the seven phylogroups A, B, C, D, E1, E2 and F of the *P. kerguelensis* complex. Significance of Fu's *Fs* is represented with asterisk: * $P < 0.05$, ** $P < 0.01$, *** $P < 0.005$; BI = Bouvet Island, EWS1 = Kapp Norvegia, EWS2 = Halley Bay, KP = Kerguelen Plateau, DS = Davis Sea, DDU = Dumont d'Urville Sea, RS = Ross Sea, AS = Amundsen Sea, WAP = West Antarctic Peninsula, SSh = South Shetland Islands, SO = South Orkney Islands, SSa = South Sandwich Islands, SG = South Georgia.

Figure S1

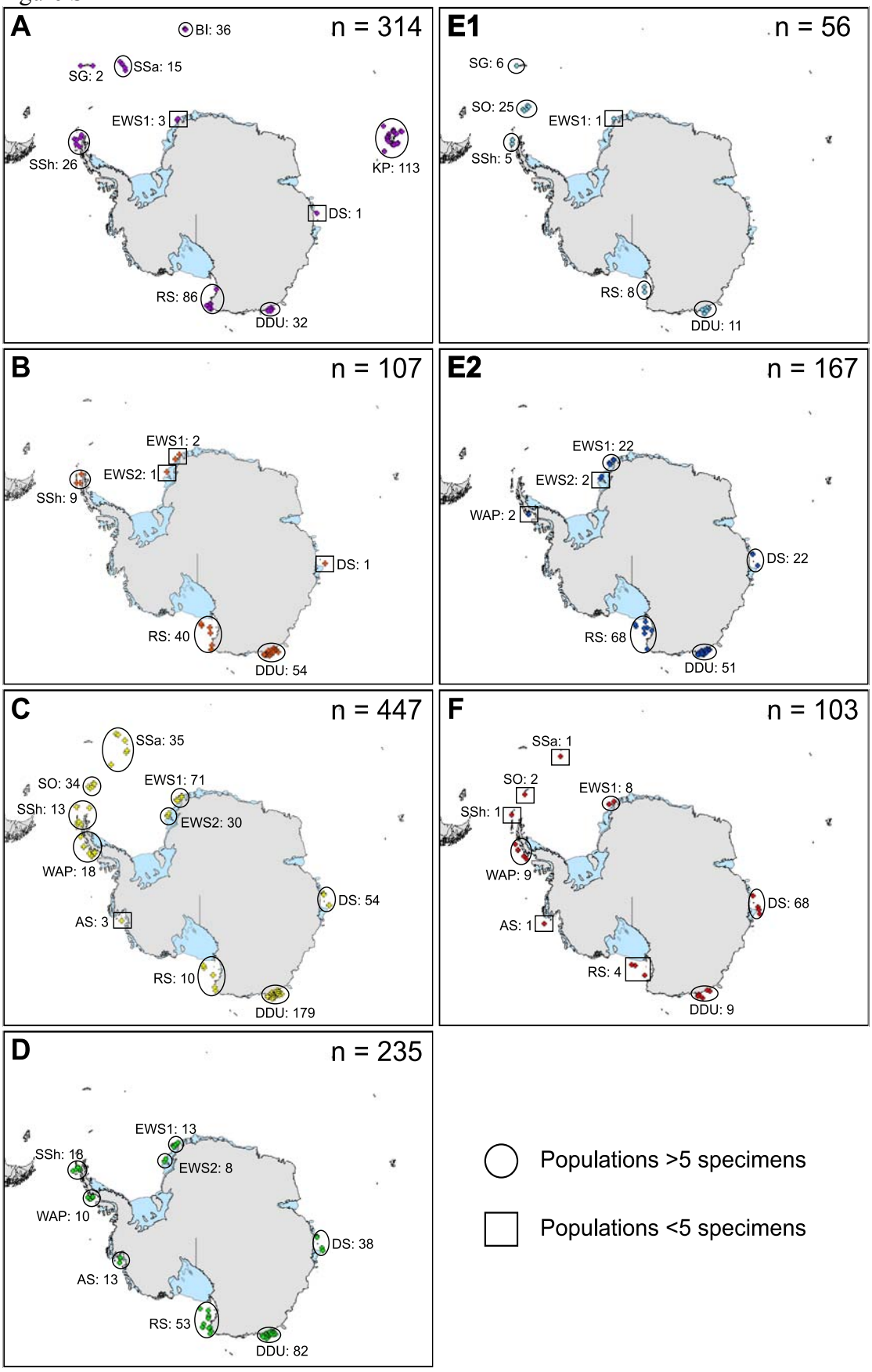
A
n = 314
BI: 36
SG: 2
SSa: 15
EWS1: 3
SSh: 26
KP: 113
DS: 1
RS: 86
DDU: 32
E1
n = 56
SG: 6
SO: 25
EWS1: 1
SSh: 5
RS: 8
DDU: 11
B
n = 107
EWS1: 2
EWS2: 1
SSh: 9
DS: 1
RS: 40
DDU: 54
E2
n = 167
EWS1: 22
EWS2: 2
WAP: 2
DS: 22
RS: 68
DDU: 51
C
n = 447
SSa: 35
SO: 34
EWS1: 71
SSh: 13
EWS2: 30
WAP: 18
DS: 54
AS: 3
RS: 10
DDU: 179
F
n = 103
SSa: 1
SO: 2
EWS1: 8
SSh: 1
WAP: 9
DS: 68
AS: 1
RS: 4
DDU: 9
D
n = 235
EWS1: 13
SSh: 18
EWS2: 8
WAP: 10
DS: 38
AS: 13
RS: 53
DDU: 82
Populations >5 specimens
Populations <5 specimens

3 Figure S2

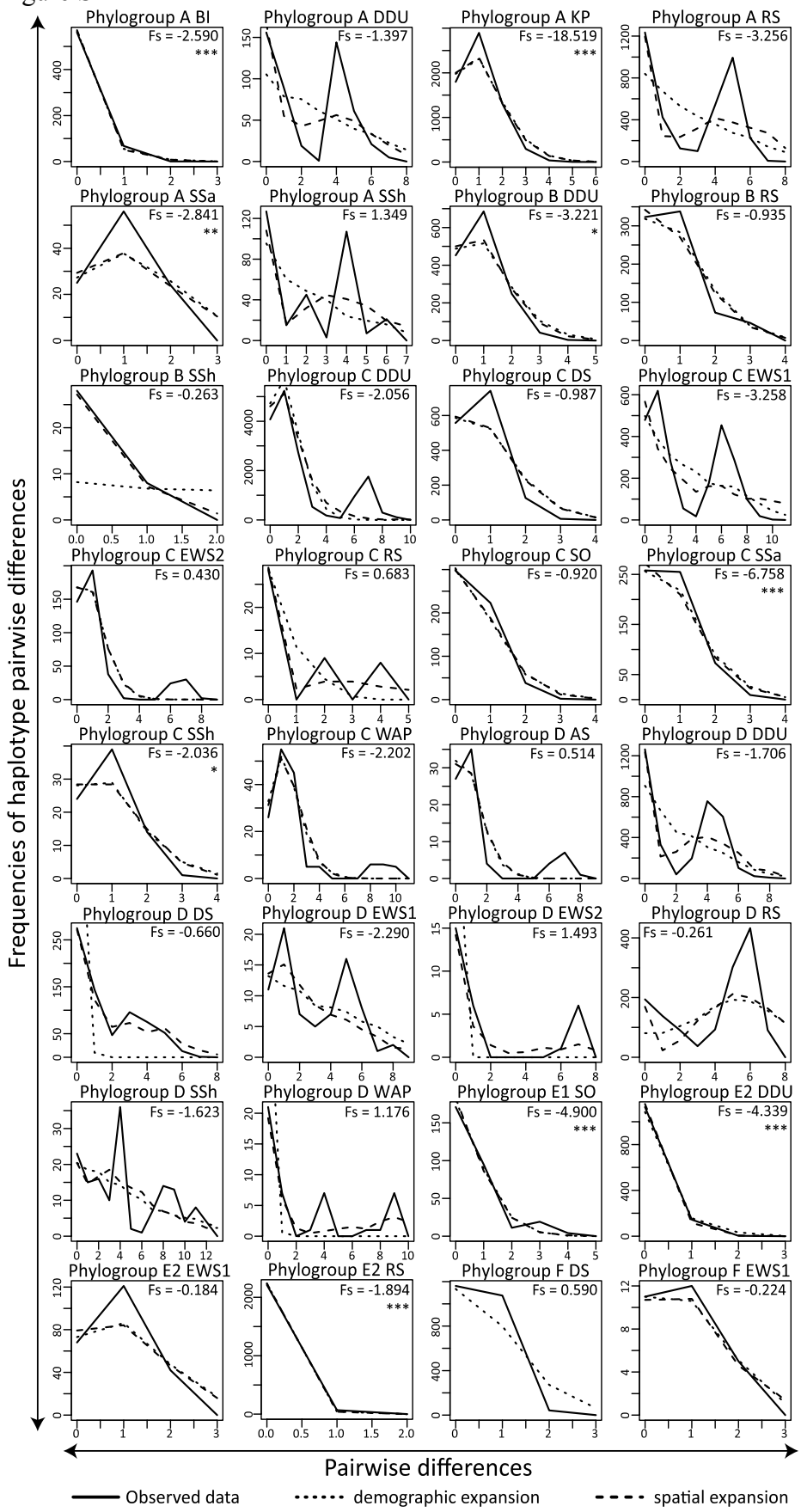
Phylogroup A BI
Fs = -2.590
***
Phylogroup A DDU
Fs = -1.397
Phylogroup A KP
Fs = -18.519
***
Phylogroup A RS
Fs = -3.256
Phylogroup A SSa
Fs = -2.841
**
Phylogroup A SSh
Fs = 1.349
Phylogroup B DDU
Fs = -3.221
*
Phylogroup B RS
Fs = -0.935
Phylogroup B SSh
Fs = -0.263
Phylogroup C DDU
Fs = -2.056
Phylogroup C DS
Fs = -0.987
Phylogroup C EWS1
Fs = -3.258
Phylogroup C EWS2
Fs = 0.430
Phylogroup C RS
Fs = 0.683
Phylogroup C SO
Fs = -0.920
Phylogroup C SSa
Fs = -6.758
***
Phylogroup C SSh
Fs = -2.036
*
Phylogroup C WAP
Fs = -2.202
Phylogroup D AS
Fs = 0.514
Phylogroup D DDU
Fs = -1.706
Phylogroup D DS
Fs = -0.660
Phylogroup D EWS1
Fs = -2.290
Phylogroup D EWS2
Fs = 1.493
Phylogroup D RS
Fs = -0.261
Phylogroup D SSh
Fs = -1.623
Phylogroup D WAP
Fs = 1.176
Phylogroup E1 SO
Fs = -4.900
***
Phylogroup E2 DDU
Fs = -4.339
***
Phylogroup E2 EWS1
Fs = -0.184
Phylogroup E2 RS
Fs = -1.894
***
Phylogroup F DS
Fs = 0.590
Phylogroup F EWS1
Fs = -0.224
Frequencies of haplotype pairwise differences
Pairwise differences
Observed data
demographic expansion
spatial expansion

4